33rd Annual International Conference of the IEEE EMBS
Boston, Massachusetts USA, August 30 - September 3, 2011

Magneto-harmonic Pressure Sensor for Biomedical Applications

Ee Lim Tan and Keat Ghee Ong, *Member, IEEE*

***Abstract*—A wireless and passive pressure sensor was developed for biomedical applications such as monitoring pressure in an abdominal aortic aneurysm sac after a stenting procedure to detect potential leakage from the stent graft. The sensor, referred to as the magneto-harmonic pressure sensor, was an airtight chamber consisting of a rigid well structure capped with an elastic membrane. A magnetically soft material was placed at the bottom of the well, while a magnetically hard material was attached to the membrane. Under the excitation of a magnetic AC field, the magnetically soft material produced a magnetic field at frequencies higher than the excitation frequency (the higher-order harmonic fields) that can be remotely detected with an external detection system. The pattern of the higher-order harmonic fields was dependent on the magnitude of the magnetic DC field produced by the magnetically hard material. When the ambient pressure varied, the membrane of the sensor deflected, changing the separation distance between the magnetically hard and soft materials. This in turn changed the magnitude of the magnetic DC field, causing a shift in the higher-order harmonic field pattern. This paper describes the design and fabrication of the sensor, and its implementation to mice to evaluate its performance in a biological environment.**

I. Introduction

A wireless and passive pressure sensor, referred to as the magneto-harmonic pressure sensor [1,2], was developed for biomedical applications. As illustrated in Fig. 1, the sensor was consisted of a magnetically soft material and a magnetically hard material. These two magnetic elements were embedded inside a pressure chamber, made of a rigid well-structured body covered with an elastic membrane. The magnetically soft material was placed at the bottom of the sensor, while the magnetically hard material was attached to the membrane. Under the excitation of a magnetic AC field, the magnetically soft material produced a magnetic field at frequencies higher than the excitation frequency (the higher-order harmonic fields) that can be remotely detected with an external receiving system. As illustrated in Fig. 2, the pattern of the higher harmonic fields was dependent on the magnetic DC field generated by the magnetically hard material. When the magneto-harmonic pressure sensor was exposed to pressure variations, the membrane of the sensor deflected, changing the separation distance between the magnetically hard and soft materials. This in turn changed the magnetic DC field to the magnetically soft material, thus shifting the higher-order harmonic field pattern. Pressure variation was tracked by measuring the shift in the field pattern.

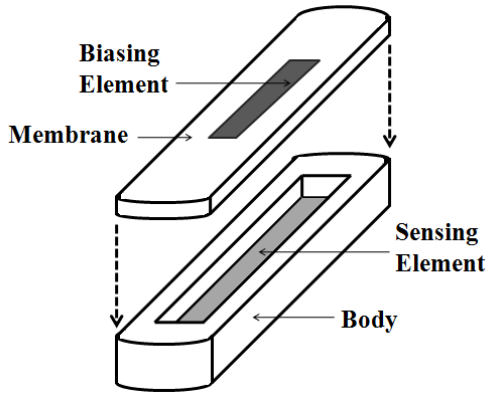

Fig. 1 A diagram illustrating the design of the magneto-harmonic pressure sensor.

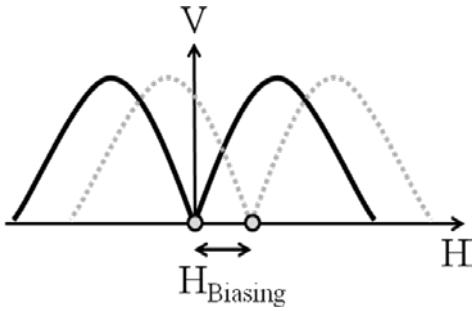

Fig. 2 The magnetic higher-order harmonic field pattern shifted when pressure variations caused the sensor membrane to deflect.

One of the biomedical applications for the magneto-harmonic pressure sensor is to monitor pressure in an abdominal aortic aneurysm (AAA) sac after a stenting procedure to detect potential leakage from the stent graft. The AAA is a localized dilation of aorta in the abdominal region due to weakening of the aortic wall. If remained untreated, AAA can grow and eventually rupture. AAA can be treated with endovascular aneurysm repair (EVAR), where a stent graft is delivered and deployed at the aneurysm site to exclude bloodstream from flowing through the weaken aorta. While this procedure is simple, 14% of patients who undergone EVAR experienced blood influx into the aneurysm site, an event known as endoleak.

Today, the computed tomography angiography remains the gold standard for postoperative surveillance of EVAR, which is both time-consuming and cost-ineffective. Another approach, which incorporates the implantable remote pressure transducer, allows for long-term surveillance of repaired aneurysm and detects endoleak. One of these pressure transducers, the Remon Impressure AAA Sac

Manuscript received March 22, 2011.

Ee Lim Tan is with the Michigan Technological University, Houghton, MI 49931 USA (e-mail: eltan@mtu.edu).

Keat Ghee Ong is with the Michigan Technological University, Houghton, MI 49931 USA (ph: 906-487-2749; e-mail: kgong@mtu.edu).

pressure transducer [3], consists of a piezoelectric membrane that charges a capacitor with ultrasound waves. Once charged, the transducer measures the sac pressure and produces an ultrasound wave that is remotely detected by a handheld probe. Since ultrasound wave does not travel through bones, incident such as calcification of AAA sac may hinder the efficacy of endoleak detection. The EndoSure Wireless AAA Pressure Sensor by CardioMEMS, Inc is another implantable pressure sensor for aneurysm sac pressure monitoring [4]. The EndoSure pressure device is based upon the inductive-capacitive resonance circuit and uses the radiofrequency energy for the power and data transmission. However, it has issues with signal strength as the attenuation of radio waves is high in the conductive human body.

Due to these complications by Impressure and EndoSure sensors, the presented magneto-harmonic pressure sensor was developed as a competing approach to monitor aneurysm sac pressure following EVAR. The magneto-harmonic pressure sensor is to be fixed on the outer surface of the stent-graft and deployed within the confinement of the aneurysm sac. The function of the pressure sensor is to detect presence of endoleak, providing a direct surveillance on the efficacy of vascular stent graft.

This paper describes the design and fabrication of the magneto-harmonic pressure sensor. The efficacy of the pressure sensor was also tested *in vitro* and *in vivo*, and the results are presented.

II. Sensor Design and Fabrication

The main components of the magneto-harmonic pressure sensor were the well-structure sensor body, the flexible membrane, the magnetically soft material (sensing element) and the magnetically hard material (biasing element).

The rigid sensor body was fabricated from MACOR glass ceramic (Corning Incorporated) due to its excellent material properties (zero porosity, non-shrinking, and hydrophobic properties), and its established application in implantable medical devices. The design of the sensor body was shown in Fig. 1. The pressure sensor body measured L_1 in length, D_1 in depth, and consisted of an arch at both ends. At center of the pressure sensor body was a rectangular well that measured L_2 in length, w in width, and depth of D_2. Here, two sizes of sensor body were fabricated, known here as Sensor I and II. For Sensor I, L_1 = 32 mm, L_2 = 28 mm, D_1 = 2.5 mm, D_2 = 2.175 mm, and w = 3 mm. For Sensor II, L_1 = 16 mm, L_2 = 13 mm, D_1 = 1.58 mm, D_2 = 1 mm, and w = 2 mm. Pressure Sensor I consisted of a larger sensor body, a design more suitable to be used in human body. Pressure Sensor II consisted of a smaller sensor body, a design suitable to be implanted in a small animal.

To ensure a great degree of membrane flexibility, a two-part medical grade silicone elastomer (Silastic® MDX4-4210 BioMedical Grade Elastomer by Dow Corning Corp.) was used as the membrane material. After mixing the silicone parts, the mixture was filled into a Teflon mold followed by putting it into a vacuum chamber to remove air bubbles. Curing was conducted in a vacuum oven at 100°C for 15 minutes. The biasing element was positioned at the center of the mold prior to filling to be embedded inside the membrane.

Commercial ferromagnetic alloy $Fe_{40}Ni_{38}Mo_4B_{18}$ (Metglas 2826MB by Metglas, Inc.) was used as the sensing element. To prepare the sensing element, a purchased 2826MB reel (28 μm thick and ½ inch wide) was sheared into 28 mm × 3 mm and 13mm × 2 mm for use in Pressure Sensor I and II, respectively, and then physically attached on the base of the well. Commercial $Fe_{60}Cr_{30}Co_{10}$ (Arnokrome™ III by Arnold Magnetic Technologies Corp.) was used as the biasing element. To prepare the biasing element, Arnokrome™ III with thickness of 40 μm was sheared into 21 mm × 2 mm and 1.27 mm × 10.16 mm for use in Pressure Sensor I and II, respectively. The biasing elements were then embedded within the pressure membrane during the casting process.

Silicone adhesive (Silbione® MED ADH 4100 RTV manufactured by Bluestar Silicones) was used to seal the pressure sensor body to the pressure membrane. Silicone adhesive was applied on the edges (width of 1.5 mm) of the pressure sensor body followed by placing the pressure membrane on the adhesive. The pressure membrane was gently pressed against the adhesive to ensure a complete contact between the bonding surfaces. The bonded surface was cured at room temperature (25°C) for 72 hours.

III. Sensor Performance Evaluation

A. In Vitro Evaluation

Fig. 3 illustrates the experimental setup used to evaluate and characterize the performance of the magneto-harmonic pressure sensor. The sensor was embedded within a conduit wall and was placed in close proximity with the excitation and receiving coils. The fluid flow was controlled by a flow/pressure regulator and the conduit pressure was measured with a commercial pressure meter. The pressure sensor was remotely excited with a 200 Hz sinusoidal signal produced by the function generator. The sensor was exposed to fluid pressures from 2 to 44 kPa (15 to 330 mmHg). At each increment of fluid pressure, the 2nd-order harmonic field was remotely acquired by the receiving coil connected to a network/spectrum analyzer.

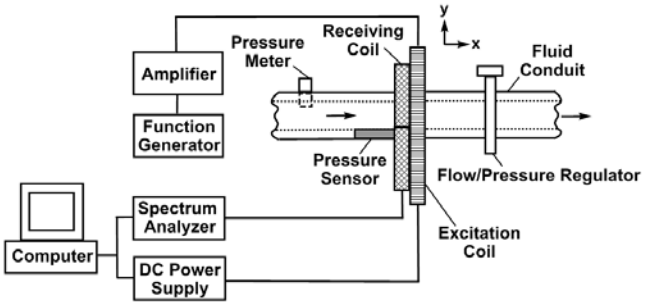

Fig. 3 The diagram illustrating the experimental setup for pressure sensor evaluation and characterization.

The harmonic shift exhibited by Pressure Sensor I and II when exposed to fluid pressure ranging 2 to 44 kPa (15 to 330 mmHg) is shown in Fig. 4. As shown, the harmonic shift increased with fluid pressure. When the surrounding pressure was increased, the sensor membrane, along with the biasing element, was deflected towards the sensing element. Since the 2nd-order harmonic shift is proportional to the DC magnetic biasing field that is exposed to the sensing element, a decreasing separation distance between these two magnetic elements caused a greater shift in the 2nd-order harmonic field. The average sensor's sensitivity, which was determined by the slope of the linear curve, was found to be 0.11949 A/m·mmHg for Sensor I and 0.2048 A/m·mmHg for Sensor II.

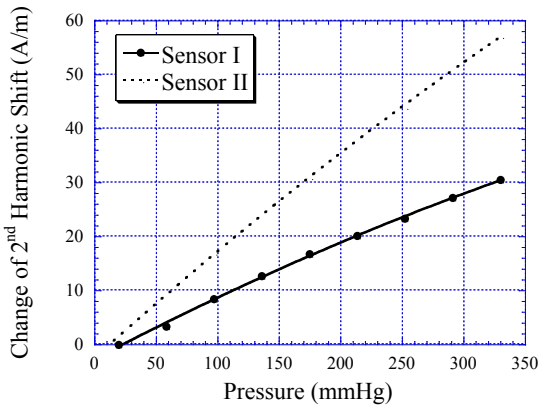

Fig. 4 The 2nd-order harmonic shift produced by Pressure Sensor I and II when exposed to varying fluid pressure of 2 to 44 kPa.

The pressure sensor's repeatability under several cycles of varying fluid pressure environment was also investigated. The fluid pressure was varied between 2 to 44 kPa. At each predetermined pressure value, the response of the pressure sensor was acquired. Both Sensor I and II exhibited good repeatability when tested for eight cycles of pressure variations. Specifically, maximum drift on the lowest detection limit exhibited by Sensor I and II were 0.87%, and 0.9%, respectively, while maximum drift on the highest detection limit on Sensor I and II were 0.48%, and 0.42%, respectively.

B. In Vivo Evaluation

Magneto-harmonic pressure sensors were implanted into mice to evaluate the sensor integrity *in vivo*. Eight male BALB/c mice with age 3 to 4 weeks were chosen as the animal model because they provided a simple reproducible model for determining the host response to an implanted composite biomaterial and that they were shown to be used as animal model in similar studies [5].

Sensor subcutaneous implantation was conducted using a previous established technique [6]. As illustrated in Fig. 5a, a small horizontal incision at the mid-lower dorsal of the mouse was made. The subcutaneous tissue was made exposed with the horizontal incision that allowed for the following vertical cut along the spine of the mouse. Then, a pouch at the left dorsal of the mouse was made by horizontally sliding a closed scissors towards the down side of the dorsal followed by opening the scissors in order to create a pocket for sensor implantation. After fixation of the sensor, the dorsal incision wound was closed using 2 surgical-grade stainless steel staples and the mouse was allowed to recover (see Fig. 5b). A photograph of the magneto-harmonic pressure sensor prior to implantation is shown in Fig. 6.

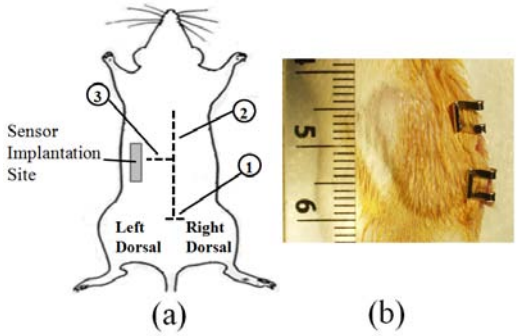

Fig. 5 (a) A schematic illustrating the dorsal view of a mouse. The pressure sensor was implanted at the left dorsal of the mouse. Three incisions were made in the process of sensor implantation. (b) Photograph image of the implanted pressure sensor at the left dorsal of the mouse.

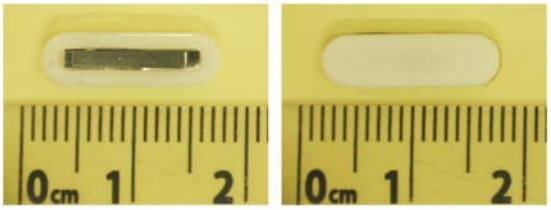

Fig. 6 The photograph of magneto-harmonic pressure sensor prior to sensor implantation.

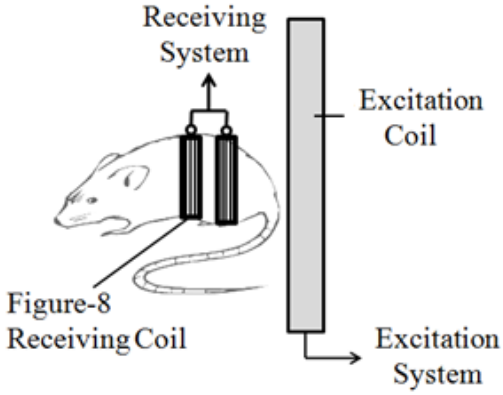

Fig. 7 Diagram illustrating the signal measurement of implanted magneto-harmonic pressure sensor using a figure-8 receiving coil.

Two time points were selected in this study for post implantation evaluations and they were 14 and 28 days. For the 14-day implantation, the response of the pressure sensor was evaluated at day-1, 3, 7, and 14 for sign of sensor signal drift. For the 28-day implantation, the response of the pressure sensor was evaluated at day-7, 14, 21, and 28. As shown in Fig. 7, a figure-8 receiving coil was worn over the torso of the mouse and was placed at the center of the excitation coil.

Fig. 8 plots the sensor drift obtained from the implanted pressure sensor in both the 14- and 28-day implantation groups (n = 3). Note that these two groups show a distinctive

curvature pattern due to the different time period when the implanted sensors were started measured (day-1 for 14-day group and day-7 for 28-day group). The data points shown in the plot illustrated an increase of the sensor drift from day-1 to 28 of implantation. It is also shown that the sensor drift was reaching plateau towards the 28-day of implantation. As compared to the full-scale output of magneto-harmonic pressure sensor, the 14- and 28-day implanted pressure sensors exhibited a percentage drift of 4.5 and 6.9 %, respectively. Given the range of pressure for the magneto-harmonic pressure sensor, the resulted sensor drift is considered small. Also, the effect of sensor drift at the early stage of implantation is believed to be negligible for the ability of the sensor to distinguish both high and low ambient pressures. Furthermore, it was demonstrated that the sensor drift became stabilized towards the 28-day of implantation. Thus, it is believed that the accuracy of pressure detection will be improved after 1 month of sensor implantation.

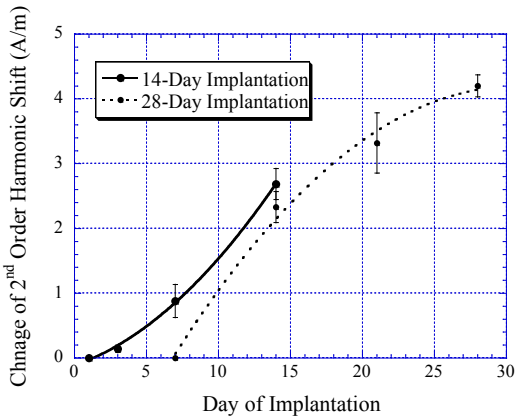

Fig. 8 The performance drift of implanted magneto-harmonic pressure sensor in 14- and 28-day implantation study groups, respectively. The 2nd-order harmonic shift of 14-day implanted sensor was measured at 1, 3, 7, and 14 day while the 28-day implanted sensor was measured at 7, 14, 21, and 28 days.

At the end of each experimental group (14- and 28-day sensor implantation), BALB/c mice were sacrificed using CO_2 asphyxiation technique and sensor explantation was performed. Compared to the non-implanted pressure sensor, there was unnoticeable tissue/fibrous formation on the surface of the sensor membrane as well as the back surface of the sensor. There was no significant host response even for the 28-day implanted sensor.

Further performance evaluation and characterization were conducted on sensors that were explanted in from the skin-tissue structure. The 2nd-order harmonic shifts produced by 14- and 28-day implanted pressure sensors are plotted in Fig. 9. The harmonic shift exhibited by non-implanted pressure sensor, referred here as the reference sensor, was used for comparison. As shown, both 14- and 28-day implanted sensors exhibited higher detection sensitivity as compared to the non-implanted sensor. It is believed that cell/tissue contraction around the body of the sensor created a pre-stressed condition to the sensor membrane, resulting in greater detection sensitivity.

The repeatability of the magneto-harmonic pressure sensor embedded within the skin-tissue structure was also evaluated and characterized. For 14-and 28-day implanted sensors, the greatest drift occurred at the 1st and 2nd cycles of pressure loading, which contributed about 8 and 4.25% of full-scale output of the sensor, respectively. It was also shown that after the 2nd cycle of pressure loading, both 14- and 28-day implanted sensor demonstrated greater stability. This finding is consistent to the results of the *in vitro* testing.

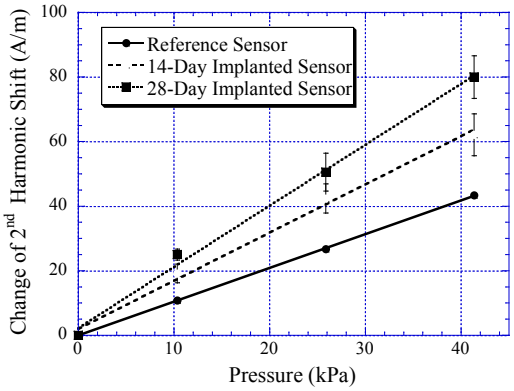

Fig. 9 The pressure characterization of magneto-harmonic pressure sensor after implantation of 14 and 28 days. Reference sensor is shown for comparison of implanted and non-implanted sensor performance.

IV. Conclusion

The efficacy and feasibility of a wireless and passive pressure sensor, known as the magneto-harmonic pressure sensor, were presented. The pressure sensor was tested *in vitro* and *in vivo*. It was demonstrated that the sensor corresponded proportionally to the ambient pressure and maintained its functionality for up to 28 days of animal implantation. Although the efficacy and feasibility of this sensor technology were demonstrated, future work such as developing a customized detection circuit and conducting *in vivo* trial on larger animals will be done to enhance the design and performance of the current pressure sensor.

References

[1] E. L. Tan, B. D. Pereles, J. Ong, K. G. Ong, "A wireless, passive strain sensor based on the harmonic response of magnetically-soft materials," *Smart Materials and Structures*, vol. 17, 025015, 2008.

[2] B. D. Pereles, E. L. Tan, K. G. Ong, "A remote query pressure sensor based on magnetic higher-order harmonic fields," *IEEE Sensors Journal*, vol. 8, 2008, pp. 1824-1829.

[3] S. H. Ellozy, A. Carroccio, R. A. Lookstein, et al, "First experience in human beings with a permanently implantable intrasac pressure transducer for monitoring endovascular repair of abdominal aortic aneurysms," *J Vasc. Surg*., vol. 40, 2004, pp. 405-412.

[4] R. A. Chaer, S. Trocciola, B. DeRubertis, et al, "Evaluation of the accuracy of a wireless pressure sensor in a canine model of retrograde-collateral (type II) endoleak and correlation with histologic analysis," *Journal of Vascular Surgery*, vol. 44, 2006, pp. 1306-1313.

[5] M. W. Laschke, A. Strohe, M. D. Menger, M. Alini, D. Eglin, "In vitro and in vivo evaluation of a novel nanosize hydroxyapatite particles/poly(ester-urethane) composite scaffold for bone tissue engineering," *Acta Biomaterialia*, vol. 6, 2010, pp. 2020-2027.

[6] P. T. Thevenot, A. M. Nair, J. Shen, P. Lotfi, C. Y. Ko, L. Tang, "The effect of incorporation of SDF-1α into PLGA scaffolds on stem cell recruitment and the inflammatory response," *Biomaterials*, vol. 31, 2010, pp. 3997-4008.